

The Coercivity Gap in Neural PDE Solvers: Parameter Escape and State Convergence

Enrique Zuazua^[1,2,3]

[1] Friedrich–Alexander–Universität Erlangen–Nürnberg, Department of Mathematics, Chair for Dynamics, Control, Machine Learning and Numerics (Alexander von Humboldt Professorship), Cauerstr. 11, 91058 Erlangen, Germany.

[2] Chair of Computational Mathematics, University of Deusto, 48007 Bilbao, Basque Country, Spain.

[3] Departamento de Matemáticas, Universidad Autónoma de Madrid, 28049 Madrid, Spain.

enrique.zuazua@fau.de

Abstract

We study variational PDE solvers based on neural-network ansatzes. In this setting, the PDE energy is minimized over a nonlinear family of realizations rather than over a linear trial space. The resulting optimization problem may have minimizing sequences for which the parameters diverge while the corresponding states remain bounded and even converge in the natural energy norm. We call this mismatch the *coercivity gap*.

We first formulate the phenomenon abstractly and then analyze a whole-space elliptic model with fixed-variance Gaussian mixtures. In this model, the relevant mechanism is the collision of two active neurons. The realized states converge to a Gaussian derivative, while the parameters escape and the reduced minimum is not attained. Under suitable regularity and decay assumptions on the forcing term, the states still converge in the energy norm, with an explicit logarithmic rate.

We also discuss measure-valued relaxations, Tikhonov regularization, residual minimization in stability norms, and a state-space HYCO formulation for hybrid physics–data problems with bounded observations.

Keywords. Neural PDE solvers; coercivity gap; state convergence; parameter escape; variational approximation; residual minimization; nonattainment; Gaussian neural networks; HYCO.

MSC 2020. 35J20; 41A30; 49J45; 65N35; 68T07.

1 Introduction

1.1 Problem formulation and main results

Physics-informed neural networks, the Deep Ritz method, and related variational or residual formulations are now widely used for partial differential equations (PDEs); see [32, 11, 19, 28, 9, 8] and the overview [2]. Their appeal is clear in high-dimensional and mesh-free settings, but replacing a linear trial space by a nonlinear realization class changes the geometry of the approximation problem: classical questions of approximation, stability, compactness, and convergence acquire new forms, because the topology that is natural for the physical state need not control the parameters of its neural representation.

The central phenomenon is the *coercivity gap*. A PDE energy may be coercive on a function space, but once it is pulled back through a nonlinear neural parametrization, compactness in

parameter space may be lost. In particular, a sequence of parameter vectors may become unbounded while the corresponding neural functions remain bounded, or even converge strongly, in the natural norm.

Figure 1 illustrates this split. The parameter sequence may escape, while the realized states remain controlled by the PDE energy. In that case, the relevant quantity to monitor is the state error, not the convergence of a particular parameter representation.

This point is important in practice. Parameter escape, large weights, or nearly colliding centers do not by themselves mean that the PDE approximation has failed. They may simply reflect an ill-conditioned or nonunique parametrization, while the computed state is already accurate in the relevant energy or residual norm. In numerical work, the state, the energy gap, the residual in a stability norm, and the data misfit are the main objects of interest; the parameters are only a way to generate them.

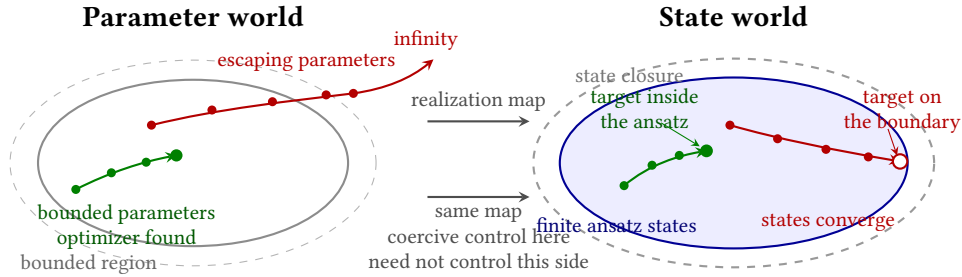


Figure 1: The coercivity gap. The algorithm searches in parameter space, while the PDE energy controls the realized state. When the target is represented inside the finite ansatz, a minimizing sequence may stay bounded. When the target is reached only as a boundary state, the realized states may converge even though the corresponding parameters escape.

This distinction can be hidden by the way the discrete problem is formulated. Some analyses introduce an auxiliary constrained or regularized parameter problem: the weights are restricted to a bounded set, compactness is imposed a priori, or a direct parameter penalty is added. Such devices are useful for proving existence or convergence, but they should not be confused with coercivity of the original PDE loss pulled back through the neural parametrization. By imposing compactness at the parameter level, they rule out parameter escape by assumption. The coercivity gap studied here concerns the untruncated realization problem, where the PDE energy controls the realized state but need not control the parameters that represent it.

We first formulate this phenomenon abstractly, and then study it for a whole-space elliptic equation with fixed-variance Gaussian mixtures. In that model the neural states converge quantitatively, while the reduced optimization problem has no minimizer and no bounded minimizing parameter sequence.

The main contributions of this paper are the following.

- (i) a Hilbert-space abstract description of the coercivity gap phenomenon;
- (ii) a whole-space, fixed-variance Gaussian construction in $H^1(\mathbb{R}^d)$: two distinct active neurons collide and converge to a Gaussian derivative outside every finite realization class; a suitable elliptic right-hand side then yields an unattained reduced infimum and forces every parameter-space minimizing sequence to escape;
- (iii) quantitative state estimates, including a constructive whole-space $O((\log P)^{-1/2})$ bound under weighted regularity, with the neuron count made explicit; and
- (iv) extensions to measure relaxation, Tikhonov regularization, residual minimization, and a HYCO-type hybrid formulation, always in norms compatible with PDE stability.

We use fixed-variance Gaussian radial-basis functions (see [4, 26, 37]) because the collision mechanism, the closure defect, and the approximation estimates can be written explicitly. No claim of architectural optimality is intended. The point is rather to show, in a model where the mechanism can be followed by hand, that parameter escape can coexist with convergence in the PDE energy norm.

Most of the ingredients are known in approximation theory and neural-network topology; see the bibliographical discussion below. The point here is to place them inside a variational, or residual, PDE setting where nonattainment and parameter escape occur together with strong state convergence.

The estimates also clarify why good state-level performance can coexist with poor parameter behavior. This gives a mathematical reason for a common computational observation: neural PDE solvers may produce reliable fields even when their weights, centers, or other coordinates are hard to interpret.

The main point is a state-space one. A neural PDE solver maps parameters to a physical field, and the PDE energy, residual, or observation loss depends on that field. Divergence or nonuniqueness of the coordinates is therefore a conditioning or identifiability issue, not a PDE error by itself. Conversely, a small training loss is meaningful for the PDE only when it is measured in a norm that controls the state.

1.2 Literature review

The parameter–realization distinction has been analyzed in the context of the existence of best neural approximants [14]. The instability of best-approximation maps, including for Gaussian radial-basis networks, was studied in [18]. For fixed architectures, [31] analyzed the nonclosedness of realization sets for broad classes of activations, the failure of inverse stability, and the resulting blow-up of weights along near-best approximation sequences when a best approximation is not attained. In [27], nonclosedness phenomena were extended to Sobolev topologies by means of two-neuron difference quotients of the form

$$n[\rho(\cdot + 1/n) - \rho(\cdot)] \longrightarrow \rho', \quad (1)$$

which provide examples of Sobolev convergence accompanied by unbounded parameter growth. This construction is the direct approximation-theoretic precursor of the collision mechanism used below. Related questions about closedness and existence of optimal parameters, in particular for sparse ReLU architectures, are studied in [21].

Here nonclosedness, nonattainment, and parameter escape are tied to a coercive elliptic energy and to the approximation of a PDE solution. At a broader analytical level, cancellation between nearby modes is also a classical device for constructing localized wave packets [41].

We also use the term *neuron condensation* in a narrower sense. In the training-dynamics literature, it usually refers to a regime in which many neurons concentrate along a small number of feature-space directions [24, 39]. The mechanism here is different. Two or more fixed-variance Gaussian centers coalesce, their signed amplitudes diverge, and the realized functions converge to a Gaussian derivative, as in (1).

A complementary line of work establishes convergence at the level of the realized physical states. For PINNs and residual minimization methods, several results prove convergence under suitable assumptions on PDE stability, regularity, sampling, approximation, and optimization [35, 9, 8]. For the Deep Ritz method, Γ -convergence and equicoercivity arguments similarly imply convergence of realizations of global quasi-minimizers [29, 10]. Coercivity and compactness have also been used as a stability framework for neural PDE approximations [13].

These works establish convergence at the state level. Our point is different. The realized states may converge strongly while the parameters representing them are noncompact or divergent. This is the parameter–state separation that the present paper isolates.

The closest PDE precedent for this parameter–state separation is [3], in the setting of weak adversarial networks (WANs). There the authors observe that neural trial classes need not be closed, analyze weakly convergent minimizing sequences, derive quasi-best-approximation bounds for the limiting states, and note that parameter norms must become unbounded when the limit does not belong to the neural class. Their work is therefore close in spirit to the mechanism studied here. The present paper formulates the issue as a variational gap between coercivity in state space and compactness in parameter space.

A separate source of ill-posedness arises when a continuous variational or residual functional is replaced by finitely many measurements. Recent work shows that quadrature-based Deep Ritz losses and weak PINN formulations can then possess nonunique or degenerate minimizers [20]. This finite-information mechanism is distinct from ours: the Gaussian collision below already causes nonattainment for the exact continuous coercive energy, before sampling or quadrature is introduced.

Measure-valued relaxed formulations give a convex way of looking at neural approximation [1, 6, 34]. The same issue persists there: unless the total variation of the representing measures is penalized, the measures may diverge while the states still converge. Indeed, the Gaussian relaxation considered below gives an explicit example of this limitation: the finite-dimensional collision disappears as a parametrization issue, but a related lack of coercivity may persist at the level of representing measures.

A related but distinct issue appears in finite element approximations of sharp Sobolev constants [15]. There the approximation spaces are linear, but the variational problem has a nonlinear manifold of minimizers, and small energy deficit must be converted into proximity to this manifold, modulo the relevant symmetries. This is different from the parameter–state coercivity gap studied here, but it reflects the same general principle that variational convergence depends on identifying the correct object of stability.

The contribution is to place this nonclosedness mechanism inside a coercive PDE energy and to quantify the resulting state convergence. This separates the physical stability estimate from the compactness, or lack of compactness, of the chosen neural parametrization.

1.3 Structure of the paper

The paper proceeds as follows. Section 2 gives the abstract stability estimates. Section 3 introduces the Gaussian elliptic model. Section 4 proves the collision, nonclosedness, and nonattainment results. State convergence and rates are proved in Section 5. Relaxation, regularization, kernel choice, residual losses, and HYCO variants are discussed in Sections 6 to 8. The appendices give the weighted spectral and localization estimates.

2 The abstract coercivity gap

2.1 An abstract setting

Let X be the physical state space, let $E : X \rightarrow \mathbb{R}$ be a convex energy, and let the nonlinear ansatz classes be generated by realization maps. For each $P \in \mathbb{N}$, we consider a parameter set Θ_P , a map

$$\Phi_P : \Theta_P \longrightarrow X,$$

and the realized class $\mathcal{A}_P := \Phi_P(\Theta_P) \subset X$. Thus, the relevant objects are organized at three distinct levels:

$$\text{parameters} \quad \longrightarrow \quad \text{realized states} \quad \longrightarrow \quad \text{energy values,}$$

or, more precisely,

$$\Theta_P \xrightarrow{\Phi_P} \mathcal{A}_P := \Phi_P(\Theta_P) \subset X \xrightarrow{E} \mathbb{R}, \quad \mathcal{L}_P := E \circ \Phi_P. \quad (2)$$

The coercivity gap appears precisely in this three-level structure. Coercivity of the physical energy E controls the realized state $\Phi_P(\Theta)$ in X , but it does not by itself control the parameter vector Θ . Thus, bounded or even vanishing energy error may imply compactness and convergence of the states, while the corresponding parameters may have no bounded subsequence. The results below separate these two effects: the abstract stability theorem explains why near-minimal energies imply convergence of realized states, whereas the nonattainment and collision results show how the associated minimizing parameters can escape.

The separation is therefore useful, not merely negative. It tells us that the right compactness question for a PDE solver is first a compactness question for the realized states. Parameter compactness is relevant for conditioning, attainment, and algorithmic robustness, but it is not the same as convergence of the numerical solution in the PDE topology. In particular, parameter escape should be read as a warning about representation and training, not as automatic evidence that the computed state is inaccurate.

More precisely, the following three questions concern different aspects of the problem and should therefore be treated separately:

- (i) *State stability*: do near-minimal reduced losses imply that $\Phi_P(\Theta)$ is close to the exact minimizer in X ?
- (ii) *Attainment and parameter compactness*: is the infimum over \mathcal{A}_P attained, and can minimizing parameters remain bounded?
- (iii) *Training*: can a given algorithm reach such near-minimal losses, and at what cost?

The next theorem addresses the first question. Under strong convexity, energy accuracy gives strong convergence of realized states. It says nothing about attainment or boundedness of parameters. In Section 4, the Gaussian collision answers the second question negatively for a concrete elliptic energy: the reduced infimum is not attained and every minimizing parameter sequence escapes.

Training dynamics are a separate issue. Our results start from global, or sufficiently near-global, minimizing sequences and analyze the behavior of their realized states in the PDE energy space. They do not explain how such sequences are produced by a particular optimizer. That question depends on the chosen algorithm, initialization, step sizes, regularization, and the nonconvex loss landscape. We therefore separate the variational mechanism of state convergence and parameter escape from the algorithmic problem of reaching the relevant near-minimal energy levels.

We assume no closedness, injectivity, or compactness of the parametrization. The only structural condition is that the realized classes are nested,

$$\mathcal{A}_P \subset \mathcal{A}_{P+1},$$

as is the case, for instance, when an additional zero-weight unit can be added.

The additional assumption used below is strong convexity, which converts an energy error into a norm error for the realized states. Recall that $E : X \rightarrow \mathbb{R}$ is λ -strongly convex if, for every $v, w \in X$ and $t \in [0, 1]$,

$$E((1-t)v + tw) \leq (1-t)E(v) + tE(w) - \frac{\lambda}{2}t(1-t)\|v - w\|_X^2.$$

The state-space argument has the usual structure of a Γ -convergence proof; see Dal Maso [7]. At that level one combines a liminf, or stability, mechanism with a recovery mechanism showing that the approximating classes envelop the limiting problem. In Galerkin methods, finite-dimensional approximation properties provide the recovery step; in neural methods, the analogous role is played by universal approximation, or more generally by density of the realization classes.

This variational picture is clear as long as it is formulated in the state space. It becomes less clear after pulling the problem back to parameters. Γ -convergence and equicoercivity in the physical topology may imply compactness and convergence of realized states, but they do not by themselves give compactness of parameter representatives. The coercivity gap is precisely this missing implication: the states may converge in the PDE energy space while the parameters used by the numerical method escape.

Parameter constraints and regularizers remove this escape mechanism by assumption. They are often useful, but they should be distinguished from coercivity of the physical loss itself.

2.2 Energy accuracy implies state accuracy

Two errors enter the estimate. The best energy value over \mathcal{A}_P measures the expressive accuracy of the class, whether or not that value is attained. A computed state generally reaches it only up to an optimization tolerance. The theorem turns these two quantities into a state-error bound.

Theorem 2.1 (State stability for nonclosed realization classes). *Let X be a Hilbert space. Let $E : X \rightarrow \mathbb{R}$ be coercive, weakly lower semicontinuous, and λ -strongly convex for some $\lambda > 0$. Let $u \in X$ denote its unique minimizer and define*

$$m_P := \inf_{v \in \mathcal{A}_P} E(v), \quad \alpha_P := m_P - E(u) \geq 0.$$

Assume that there are $a_P \in \mathcal{A}_P$ such that

$$a_P \rightarrow u \quad \text{in } X, \quad E(a_P) \rightarrow E(u).$$

Then:

(a) *The best energy errors satisfy*

$$0 \leq \alpha_P \leq E(a_P) - E(u) \rightarrow 0. \quad (3)$$

(b) *If $v_P \in \mathcal{A}_P$ satisfies*

$$E(v_P) \leq m_P + \varepsilon_P, \quad \varepsilon_P \geq 0,$$

then

$$\|v_P - u\|_X^2 \leq \frac{2}{\lambda}(\alpha_P + \varepsilon_P). \quad (4)$$

In particular, $v_P \rightarrow u$ strongly in X whenever $\varepsilon_P \rightarrow 0$.

(c) For fixed P , every minimizing sequence $(v_P^k)_k \subset \mathcal{A}_P$ is bounded in X . If \bar{v}_P is any of its weak accumulation points, then

$$E(\bar{v}_P) \leq m_P, \quad \|\bar{v}_P - u\|_X^2 \leq \frac{2}{\lambda} \alpha_P. \quad (5)$$

Thus every selection of fixed- P relaxed accumulation states converges strongly to u as $P \rightarrow \infty$.

These conclusions do not require bounded or convergent parameters, or attainment of m_P in \mathcal{A}_P .

Proof. Strong convexity and minimality of u imply

$$E(v) - E(u) \geq \frac{\lambda}{2} \|v - u\|_X^2, \quad v \in X. \quad (6)$$

Indeed, apply strong convexity to $(1-t)u + tv$, use the minimality of u , and let $t \downarrow 0$.

Since $E(u) \leq m_P \leq E(v_P)$, the approximation hypothesis gives (3). For the near-minimizers in part (b),

$$\frac{\lambda}{2} \|v_P - u\|_X^2 \leq E(v_P) - E(u) \leq \alpha_P + \varepsilon_P,$$

which proves (4).

For part (c), coercivity makes each fixed-width minimizing sequence bounded. Hilbert-space weak compactness then provides a weakly convergent subsequence. Weak lower semicontinuity gives $E(\bar{v}_P) \leq m_P$. Consequently,

$$\frac{\lambda}{2} \|\bar{v}_P - u\|_X^2 \leq E(\bar{v}_P) - E(u) \leq \alpha_P,$$

which proves (5). □

Remark 2.2 (The state-error estimate and the scope of the theorem). *Estimate (4) should be read as a state-space estimate with the following features:*

- It depends only on the class approximation error α_P and on the optimization tolerance ε_P .
- It contains no bound on the parameter norm and no conditioning estimate for the neural parametrization.
- It assumes access to a global near-minimal energy level. Thus, it does not address the algorithmic question of how such a near-minimizer is found.
- In particular, the result does not make the pulled-back loss \mathcal{L}_P convex in the parameters and does not analyze gradient descent.
- Strong convexity is used only at the level of the physical energy. Its role is to convert a small energy gap into a direct norm estimate for the realized state.
- More general Γ -convergence arguments can yield qualitative convergence under weaker assumptions. The quadratic elliptic energy considered below provides the sharper identity needed for the explicit error bound.

2.3 Nonattainment and parameter escape

Theorem 2.1 remains valid when \mathcal{A}_P is nonclosed. A fixed-width minimizing sequence then has weak accumulation points in the weak closure of \mathcal{A}_P , but those relaxed states need not belong to \mathcal{A}_P . In the Gaussian collision below the convergence is strong, and the limit lies in $\overline{\mathcal{A}_P}^X \setminus \mathcal{A}_P$. The PDE energy still controls the states, while the reduced parameter problem may have no minimizer. In finite dimensions, this forces parameter escape.

Proposition 2.3 (Nonattainment forces parameter escape). *Fix P , let $\Theta_P = \mathbb{R}^{N_P}$, and suppose that $\Phi_P : \Theta_P \rightarrow X$ and $E : X \rightarrow \mathbb{R}$ are continuous. If*

$$\inf_{\Theta \in \Theta_P} E(\Phi_P(\Theta)) = m_P$$

is not attained, then every parameter-space minimizing sequence $(\Theta_k)_k$ satisfies $\|\Theta_k\| \rightarrow \infty$.

Proof. If $\|\Theta_k\| \not\rightarrow \infty$, a subsequence lies in a bounded subset of \mathbb{R}^{N_P} . It has a further convergent subsequence, $\Theta_{k_\ell} \rightarrow \Theta_*$. Continuity then yields

$$E(\Phi_P(\Theta_*)) = \lim_{\ell \rightarrow \infty} E(\Phi_P(\Theta_{k_\ell})) = m_P,$$

contradicting nonattainment. □

The converse is false: parameters can diverge because of redundant representations even when a minimizer exists. This is why Section 4 removes inactive-neuron, permutation, and repeated-center explanations and constructs a collision of two distinct active neurons. Its nonattainment result is the architecture-specific complement to the architecture-independent state theorem above.

The abstract framework will be instantiated in the next sections by a whole-space elliptic equation and a fixed-variance Gaussian realization class. There, $X = H^1(\mathbb{R}^d)$, the energy is the elliptic functional J , and the realization map sends weights and centers to Gaussian mixtures. In that model, the identity

$$J(v) - J(u) = \frac{1}{2} \|v - u\|_{H^1}^2$$

makes the state stability mechanism completely explicit, while the Gaussian collision construction shows that the corresponding parameter problem may have no minimizer and that every minimizing parameter sequence escapes.

2.4 Residual losses

The same principle underlying the coercivity gap also appears in residual formulations. What is needed for state convergence is a lower stability estimate for the residual in the norm in which the PDE error is measured. After this state-space estimate has been fixed, approximation and optimization errors enter the error bound, but no corresponding coercive control of the neural parameters is implied.

Proposition 2.4 (Abstract stable-residual estimate). *Let X and Y be Hilbert spaces, let $B : X \rightarrow Y$ be bounded, and assume that*

$$\|z\|_X \leq C_B \|Bz\|_Y, \quad z \in X. \tag{7}$$

For $g = Bu$, define

$$\mathcal{R}_B(v) := \|Bv - g\|_Y^2, \quad d_P := \inf_{w \in \mathcal{A}_P} \|w - u\|_X.$$

If $v_P \in \mathcal{A}_P$ satisfies

$$\mathcal{R}_B(v_P) \leq \inf_{w \in \mathcal{A}_P} \mathcal{R}_B(w) + \eta_P, \quad \eta_P \geq 0,$$

then

$$\|v_P - u\|_X \leq C_B(\|B\|d_P + \sqrt{\eta_P}). \quad (8)$$

In particular, $v_P \rightarrow u$ in X whenever $d_P \rightarrow 0$ and $\eta_P \rightarrow 0$, irrespective of parameter compactness.

Proof. By stability and near-minimality,

$$\begin{aligned} \|v_P - u\|_X &\leq C_B \mathcal{R}_B(v_P)^{1/2} \\ &\leq C_B \left(\inf_{w \in \mathcal{A}_P} \|B(w - u)\|_Y^2 + \eta_P \right)^{1/2} \\ &\leq C_B(\|B\|d_P + \sqrt{\eta_P}). \end{aligned}$$

□

Remark 2.5 (Choice of residual norm). *The residual must be measured in a norm that controls the state error. The essential PDE input is a stability estimate of the form*

$$\|v - u\|_X \leq C\|Bv - f\|_Y.$$

Thus the residual space Y is not arbitrary: it has to be chosen so that this estimate is valid.

For a second-order elliptic problem, an H^{-1} residual naturally controls the error in H^1 . By contrast, an L^2 residual is tied to an H^2 -regularity framework. It controls an H^2 -type error only when the trial functions belong to the domain of the operator as a map into L^2 , and when the corresponding elliptic regularity estimate holds for the domain, coefficients, and boundary conditions under consideration.

If B has a nontrivial kernel, the residual controls only the distance to the solution set. Boundary conditions, normalization constraints, or other side conditions are then needed to recover uniqueness. For nonlinear operators, the same principle applies, but the stability estimate is usually conditional: it must hold on the part of the state space reached by the minimizing sequence.

If boundary or initial conditions are imposed through the loss, they must be included in the residual norm, leading to a product-space formulation. These are the alternatives developed in Section 8.

3 An elliptic model and a Gaussian realization class

3.1 A coercive elliptic energy and nonclosed Gaussian classes

We consider

$$-\Delta u + u = f \quad \text{in } \mathbb{R}^d, \quad (9)$$

where $f \in H^{-1}(\mathbb{R}^d)$. We use the energy norm

$$\|v\|_{H^1}^2 := \int_{\mathbb{R}^d} (|\nabla v|^2 + |v|^2) dx$$

and its associated dual norm. The weak solution $u \in H^1(\mathbb{R}^d)$ is the unique minimizer of

$$J(v) := \frac{1}{2} \|v\|_{H^1}^2 - \langle f, v \rangle_{H^{-1}, H^1}. \quad (10)$$

Since u solves (9),

$$J(v) - J(u) = \frac{1}{2} \|v - u\|_{H^1}^2, \quad v \in H^1(\mathbb{R}^d). \quad (11)$$

Thus J is coercive and 1-strongly convex.

When J is restricted to a closed finite-dimensional linear Galerkin space, these properties ensure a unique discrete minimizer and imply the usual best-approximation stability estimate. The issue studied here arises because a nonlinear realization class need not be linear or closed: coercivity of J controls the state norm but does not make parameter sublevels compact.

Let

$$G(x) := (4\pi)^{-d/2} e^{-|x|^2/4}, \quad \widehat{G}(\xi) = e^{-|\xi|^2}, \quad (12)$$

where $\widehat{v}(\xi) = \int_{\mathbb{R}^d} e^{-ix \cdot \xi} v(x) dx$. For $P \geq 1$, define the realization map

$$\Phi_P(\Theta)(x) := \sum_{j=1}^P w_j G(x - x_j), \quad \Theta = ((w_j, x_j))_{j=1}^P \in \mathbb{R}^{P(d+1)}, \quad (13)$$

and its image

$$\mathcal{M}_P := \Phi_P(\mathbb{R}^{P(d+1)}) \subset H^1(\mathbb{R}^d).$$

Although the parameter space has dimension $P(d+1)$, \mathcal{M}_P is not a smooth manifold globally: permutations, vanishing weights, repeated centers, and weight splitting create singular strata and nonunique representations. We therefore call \mathcal{M}_P a *realization class*.

For example, if two centers coincide, then

$$aG(\cdot - x) + bG(\cdot - x) = (a+b)G(\cdot - x),$$

so the two parameter vectors $((a, x), (b, x))$ and $((a+b, x), (0, y))$ represent the same element of \mathcal{M}_P , for any $y \in \mathbb{R}^d$. Similarly, permuting the neurons or changing the center of a zero-weight neuron does not change the realized function.

Set

$$I := J(u), \quad I_P := \inf_{v \in \mathcal{M}_P} J(v) = \inf_{\Theta \in \mathbb{R}^{P(d+1)}} J(\Phi_P(\Theta)). \quad (14)$$

The classes are nested because zero-weight neurons may be added. Finite linear combinations of translates of G are dense in $H^1(\mathbb{R}^d)$, a consequence of Wiener's Tauberian theorem [38]. Hence

$$I_P \downarrow I. \quad (15)$$

The reduced infimum I_P need not, however, be attained.

Remark 3.1 (Fixed variance). *In the present ansatz, only the centers and output weights are allowed to vary; the Gaussian variance is kept fixed. This restriction is intentional. It gives a simple realization class in which the collision mechanism can be isolated without additional degeneracies.*

The fixed variance may, of course, be inefficient when the target function has a very different characteristic scale. Allowing trainable variances would enlarge the approximation class and could improve efficiency. At the same time, it would introduce further noncompactness mechanisms, such as dilation or concentration of the Gaussian profiles. These scale-related degeneracies are not analyzed here.

3.2 Dictionary with the abstract coercivity-gap framework

The abstract objects of Section 2 specialize in the present Gaussian elliptic model as follows:

Abstract object	Gaussian elliptic model
X	$H^1(\mathbb{R}^d)$
E	the elliptic energy J in (10)
u	the solution of $-\Delta u + u = f$
Θ_P	P weights and P centers in $\mathbb{R}^{P(d+1)}$
\mathcal{A}_P	the Gaussian realization class \mathcal{M}_P
m_P	the reduced infimum I_P
α_P	$I_P - I$, the best energy error

For this concrete problem, the strong-convexity estimate of Theorem 2.1 becomes the exact identity (11). Thus the abstract coercivity gap takes a particularly transparent form: the elliptic energy controls convergence of the realized Gaussian states in $H^1(\mathbb{R}^d)$, while the reduced parameter problem may fail to attain its infimum and its minimizing parameter sequences may escape.

3.3 Comparison with Galerkin approximations

The contrast with a classical Galerkin discretization can be stated exactly for the quadratic model. Let $V \subset H^1(\mathbb{R}^d)$ be a closed linear trial space. The minimizer $u_V \in V$ is characterized by

$$(u - u_V, v)_{H^1} = 0, \quad v \in V, \quad (16)$$

and is therefore the H^1 -orthogonal projection of u onto V . Consequently,

$$\|u - u_V\|_{H^1} = \inf_{v \in V} \|u - v\|_{H^1}. \quad (17)$$

The discrete problem has a unique state minimizer, even though a chosen basis may still introduce an algebraic conditioning issue.

For a general realization class $\mathcal{A} \subset H^1$, linearity is not needed to identify the infimum. Identity (11) gives

$$\inf_{v \in \mathcal{A}} J(v) - J(u) = \frac{1}{2} \text{dist}_{H^1}(u, \mathcal{A})^2. \quad (18)$$

The projection mechanism is lost: a best approximant need not exist, need not be unique, and no Galerkin orthogonality is available. In the Gaussian example of Section 4, the distance is zero although the target does not belong to the class, so the reduced energy infimum equals the exact minimum but is not attained. Approximation accuracy, state well-posedness, parameter identifiability, and conditioning are therefore separate questions.

Remark 3.2 (Fixed centers and random features). *If the centers x_1, \dots, x_P are fixed in advance, then the ansatz reduces to the linear space*

$$V_P(x_1, \dots, x_P) = \text{span}\{G(\cdot - x_j) : 1 \leq j \leq P\}.$$

This includes, for instance, random-feature-type constructions, where the centers are sampled and then kept fixed. In that setting the only trainable variables are the output weights, and the minimization problem is linear quadratic. The weights are determined by a positive-definite Gram system, provided the fixed centers are distinct.

This fixed-center problem can still be numerically ill-conditioned: if two centers are very close, the corresponding Gaussian translates are nearly linearly dependent. However, this is a conditioning issue inside a fixed linear space, not the nonclosedness mechanism studied here.

The coercivity gap considered in this paper appears when the centers are also trained. Then the realization class itself can approach collision configurations, and the reduced infimum may fail to be attained. Thus training the centers adds adaptivity, but it also opens the door to parameter escape.

A more quantitative analysis of this mechanism, including the dependence of the Gram matrices on the centers and their degeneration near collision configurations, is being developed in the work in preparation [12].

4 Collision, nonclosedness, and nonattainment

The following collision is not a mere redundancy of the parametrization. The two neurons remain active and distinct for every $h > 0$, but their realized states converge to a limit outside the finite Gaussian realization class. Thus the relevant geometric fact is nonclosedness in the state topology: $\partial_1 G$ belongs to the H^1 -closure of \mathcal{M}_P , but not to \mathcal{M}_P itself, for any finite $P \geq 2$. In the elliptic example below the exact PDE solution is chosen precisely on this boundary. The reduced loss can therefore be driven down to the exact energy level, but no finite parameter vector realizes the limiting state.

Let $e_1 = (1, 0, \dots, 0)$ and, for $h > 0$, set

$$q_h(x) := \frac{G(x + he_1) - G(x - he_1)}{2h}. \quad (19)$$

Then q_h is a two-neuron realization with nonzero weights $\pm(2h)^{-1}$, distinct centers $\mp he_1$, and barycenter zero. In one space dimension this collision has the simple state-space picture shown in Figure 2: the parameter weights blow up, but the realized functions approach the smooth derivative G' .

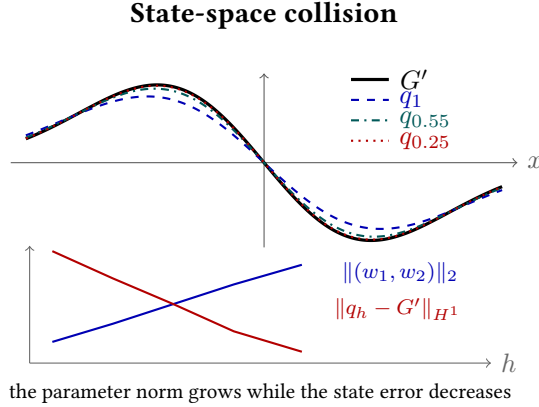


Figure 2: The explicit collision in state space for $d = 1$. The two-neuron difference quotient $q_h = (G(\cdot + h) - G(\cdot - h))/(2h)$ approaches the smooth state G' as the centers collapse and the weights grow like h^{-1} . The lower panel makes the same point quantitatively: the parameter norm increases while the state error decreases.

Proposition 4.1 (Nondegenerate collision). *As $h \downarrow 0$,*

$$q_h \longrightarrow \partial_1 G \quad \text{strongly in } H^1(\mathbb{R}^d),$$

whereas $\partial_1 G \notin \mathcal{M}_P$ for every finite P . Consequently, \mathcal{M}_P is not closed in $H^1(\mathbb{R}^d)$ for any $P \geq 2$. The parameter norm of (19) diverges even after quotienting by permutations, and the sequence uses neither inactive nor repeated neurons.

Proof. The convergence is the centered finite-difference formula in H^1 ; it also follows by dominated convergence after Fourier transformation. If $\partial_1 G \in \mathcal{M}_P$, division of the Fourier identity by the nowhere-zero \widehat{G} would give

$$i\xi_1 = \sum_{j=1}^P w_j e^{-ix_j \cdot \xi}.$$

On the line $\xi = te_1$, the right-hand side is bounded for real t , while the left-hand side is unbounded. This contradiction proves $\partial_1 G \notin \mathcal{M}_P$. The two weights have Euclidean norm $(\sqrt{2}h)^{-1}$, which diverges and is unchanged by permutation. \square

The collision also produces nonattainment.

Theorem 4.2 (Nonattainment and parameter escape). *Let*

$$u = \partial_1 G, \quad f = (-\Delta + I)\partial_1 G.$$

Then f is a Schwartz function and, for every $P \geq 2$,

$$I_P = I, \quad \operatorname{argmin}_{v \in \mathcal{M}_P} J(v) = \emptyset.$$

Every parameter-space minimizing sequence satisfies $\|\Theta^k\| \rightarrow \infty$. For $P = 2$, the explicit sequence in (19) is nondegenerate in the sense described above.

Proof. By Theorem 4.1 and the continuity of J , $J(q_h) \rightarrow J(u) = I$, so $I_P = I$ for every $P \geq 2$. If the infimum were attained by $v \in \mathcal{M}_P$, (11) would imply $v = u$, contradicting $u \notin \mathcal{M}_P$.

Parameter escape follows from Theorem 2.3: here $\Theta_P = \mathbb{R}^{P(d+1)}$, the realization map Φ_P is continuous into H^1 , and J is continuous. \square

Remark 4.3 (Boundary search at fixed width). *Theorem 4.2 should be read as a boundary-search statement. For each finite width $P \geq 2$, the target state $u = \partial_1 G$ lies on the H^1 -boundary of the nonclosed realization class \mathcal{M}_P , but not in \mathcal{M}_P . Increasing P by any finite amount does not remove this obstruction: the same state is outside every finite class \mathcal{M}_P , while the two-neuron collision sequence, padded with zero weights, belongs to every larger class. Thus the reduced infimum is the exact energy value for every finite P , but it is never attained.*

Consequently, an unregularized parameter search that keeps trying to minimize the exact reduced loss has no finite optimizer to find. In this variational sense it is forced to chase the boundary, with centers colliding and weights blowing up. This does not mean that a computation should follow the path to arbitrarily large parameters. On the contrary, the state error is already small for moderately small h , and an effective implementation would stop once the state, residual, or energy tolerance is reached, or would regularize the parameters. What fails is the naive expectation that exact minimization at fixed width should converge to a bounded parameter vector.

Remark 4.4 (Interior and boundary targets). *The example is positional. It should not be read as saying that finite Gaussian ansatzes must always exhibit parameter escape. If the exact state already belongs to \mathcal{M}_P , then the reduced minimum is attained and no boundary chase is forced. For instance, a single fixed-variance Gaussian translate is represented exactly with $P = 1$, and a finite linear combination of N such translates is represented exactly for every $P \geq N$, after padding by zero weights. In those cases the elliptic energy has an exact realized minimizer, although the parametrization may still be nonunique.*

The divergence in Theorem 4.2 occurs because the chosen PDE solution lies in the H^1 -closure of every finite realization class \mathcal{M}_P , but not in any \mathcal{M}_P itself. The ansatz has enough expressive power

to approach the state arbitrarily well, but only by moving toward a boundary point with no finite parameter representative. This is the usual role of such examples in numerical analysis: they identify a mechanism by which a method can fail at the parameter level, not a claim that every target state or every computation must diverge.

The distinction can be summarized as follows: an interior target may be reached by bounded parameters, while a boundary target may be approached in state space only through parameters that escape.

A two-neuron computation

For $d = 1$, Plancherel's identity gives the exact error formula

$$\|q_h - G'\|_{H^1(\mathbb{R})}^2 = \frac{1}{2\pi} \int_{\mathbb{R}} (1 + \xi^2) \left(\frac{\sin(h\xi)}{h} - \xi \right)^2 e^{-2\xi^2} d\xi. \quad (20)$$

For the right-hand side in Theorem 4.2, the energy gap is one half of this quantity. Table 1 reports direct quadrature of (20). The table isolates the coercivity gap from any training dynamics: the weight norm grows like h^{-1} , whereas the state error is $O(h^2)$ and the energy gap is $O(h^4)$.

Table 1: Two active neurons approaching G' in one dimension.

h	$\ (w_1, w_2)\ _2$	$\ q_h - G'\ _{H^1}$	$J(q_h) - J(G')$
0.50000	1.414214	1.45609×10^{-2}	1.06010×10^{-4}
0.25000	2.828427	3.71097×10^{-3}	6.88567×10^{-6}
0.12500	5.656854	9.32243×10^{-4}	4.34539×10^{-7}
0.06250	11.313708	2.33343×10^{-4}	2.72246×10^{-8}
0.03125	22.627417	5.83535×10^{-5}	1.70257×10^{-9}

Regularization along the collision path

The same example quantifies the bias–stability tradeoff created by a total-variation penalty. In one dimension, the Fourier representation gives

$$\widehat{q}_h(\xi) = i \frac{\sin(h\xi)}{h} e^{-\xi^2}, \quad \widehat{G}'(\xi) = i\xi e^{-\xi^2}.$$

Taylor expansion under the integrable weight in (20) yields

$$\|q_h - G'\|_{H^1}^2 = C_G h^4 + O(h^6), \quad h \downarrow 0, \quad (21)$$

where

$$C_G := \frac{1}{72\pi} \int_{\mathbb{R}} (1 + \xi^2) \xi^6 e^{-2\xi^2} d\xi > 0. \quad (22)$$

Indeed, $\sin(h\xi)/h - \xi = -h^2\xi^3/6 + O(h^4\xi^5)$, and dominated convergence applies after squaring.

For the representing measure $\mu_h = (\delta_{-h} - \delta_h)/(2h)$, one has $\|\mu_h\|_{\text{TV}} = h^{-1}$. Along this collision path, the regularized functional (41), introduced below, therefore satisfies

$$J_\delta(\mu_h) - J(G') = \frac{C_G}{2} h^4 + \delta h^{-2} + O(h^6). \quad (23)$$

Balancing the two leading terms gives

$$h_\delta \asymp \delta^{1/6}, \quad \|\mu_{h_\delta}\|_{\text{TV}} \asymp \delta^{-1/6}, \quad \|q_{h_\delta} - G'\|_{H^1} \asymp \delta^{1/3}. \quad (24)$$

Thus every fixed $\delta > 0$ prevents the singular limit, but the parameter norm again diverges as the regularization is removed. These powers describe the explicit collision family; they are not asserted to be optimal rates for the global regularized problem.

5 State convergence and quantitative Gaussian approximation

5.1 State convergence

Define the best-approximation error

$$\delta_P := \inf_{v \in \mathcal{M}_P} \|u - v\|_{H^1(\mathbb{R}^d)}. \quad (25)$$

In the notation of Section 3.2, $\alpha_P = I_P - I$. The energy identity (11) converts the abstract estimate (4) into a sharp best-approximation bound for this model.

Theorem 5.1 (State convergence and optimization error). *Let $f \in H^{-1}(\mathbb{R}^d)$, and let u solve (9).*

(a) *For fixed P , let $(v_P^k)_k \subset \mathcal{M}_P$ satisfy $J(v_P^k) \rightarrow I_P$, and let u_P be any weak H^1 -accumulation point. Then*

$$\|u_P - u\|_{H^1} \leq \delta_P. \quad (26)$$

In particular, every such selection satisfies $u_P \rightarrow u$ strongly in $H^1(\mathbb{R}^d)$ as $P \rightarrow \infty$.

(b) *If $v_P \in \mathcal{M}_P$ is a diagonal family of near-minimizers satisfying*

$$J(v_P) \leq I_P + \varepsilon_P, \quad \varepsilon_P \geq 0,$$

then

$$\|v_P - u\|_{H^1}^2 \leq \delta_P^2 + 2\varepsilon_P. \quad (27)$$

Thus $v_P \rightarrow u$ strongly whenever $\delta_P \rightarrow 0$ and $\varepsilon_P \rightarrow 0$.

Proof. Coercivity makes $(v_P^k)_k$ bounded. Weak lower semicontinuity and (11) give

$$\frac{1}{2} \|u_P - u\|_{H^1}^2 = J(u_P) - I \leq I_P - I \leq \frac{1}{2} \delta_P^2,$$

which proves (26). Wiener's theorem gives $\delta_P \rightarrow 0$. For part (b),

$$\frac{1}{2} \|v_P - u\|_{H^1}^2 = J(v_P) - I \leq I_P - I + \varepsilon_P \leq \frac{1}{2} \delta_P^2 + \varepsilon_P.$$

□

Remark 5.2. *At fixed width, u_P may lie in $\overline{\mathcal{M}_P}^{H^1} \setminus \mathcal{M}_P$. It is a relaxed physical state, not necessarily the realization of a finite parameter vector. The diagonal estimate (27) avoids selecting weak limits and is the more direct statement for computed near-minimizers.*

5.2 The weighted spectral estimate

We next bound δ_P explicitly. The proof combines Hermite spectral truncation, finite-difference realization of the resulting Gaussian jet, and a localization step.

Set

$$K(x) := e^{|x|^2/4}$$

and, for $m \in \mathbb{N}$, define

$$H^m(K) := \left\{ v \in H^m(\mathbb{R}^d) : \sum_{|\alpha| \leq m} \int_{\mathbb{R}^d} |D^\alpha v|^2 K \, dx < \infty \right\}.$$

Consider the self-adjoint operator in $L^2(K \, dx)$

$$\mathcal{L}v = -\Delta v - \frac{x \cdot \nabla v}{2} = -K^{-1} \operatorname{div}(K \nabla v). \quad (28)$$

Its eigenspaces are spanned by derivatives of $e^{-|x|^2/4} = (4\pi)^{d/2} G$, and the eigenvalue corresponding to total derivative order n is $(d+n)/2$. These eigenfunctions form an orthogonal basis in the relevant weighted Sobolev scales; see [42].

Let Π_L denote the spectral projection onto total derivative order at most L . The standard spectral tail estimate is

$$\|v - \Pi_L v\|_{H^1(K)} \leq C_d (L+1)^{-1/2} \|v\|_{H^2(K)}. \quad (29)$$

For completeness, if $v = \sum_{n \geq 0} \pi_n v$ is the orthogonal spectral expansion and $\mu_n = (d+n)/2$, the quadratic-form identity for \mathcal{L} and the weighted elliptic estimate give

$$\|v\|_{H^1(K)}^2 \asymp_d \sum_{n \geq 0} (1 + \mu_n) \|\pi_n v\|_{L^2(K)}^2, \quad \sum_{n \geq 0} (1 + \mu_n)^2 \|\pi_n v\|_{L^2(K)}^2 \leq C_d \|v\|_{H^2(K)}^2.$$

Restricting the first sum to $n > L$ and using $(1 + \mu_n) \leq (1 + \mu_{L+1})^{-1} (1 + \mu_n)^2$ proves (29). This also makes explicit why its exponent is $-1/2$. The range of Π_L is

$$V_L := \operatorname{span}\{D^\alpha G : |\alpha| \leq L\}, \quad N_L := \dim V_L = \binom{L+d}{d}.$$

It remains to represent Gaussian derivatives by a fixed number of Gaussian translates.

Lemma 5.3 (Realization of a Gaussian jet by colliding translates). *For every $L \geq 0$,*

$$V_L \subset \overline{\mathcal{M}_{N_L} H^1(\mathbb{R}^d)}.$$

More precisely, for every $q \in V_L$, there are N_L fixed, distinct vectors z_1, \dots, z_{N_L} and coefficients $c_j(h)$ such that

$$q_h(x) := \sum_{j=1}^{N_L} c_j(h) G(x - h z_j) \longrightarrow q \quad \text{in } H^1(\mathbb{R}^d) \quad \text{as } h \downarrow 0.$$

The coefficients may grow as $O(h^{-L})$.

Proof. Choose N_L points $z_j \in \mathbb{R}^d$ that are unisolvent for polynomials of total degree at most L . Thus the multivariate Vandermonde matrix $(z_j^\alpha)_{|\alpha| \leq L, 1 \leq j \leq N_L}$ is invertible. Write $q = \sum_{|\alpha| \leq L} a_\alpha D^\alpha G$ and choose the coefficients $c_j(h)$ to solve the moment equations

$$\sum_{j=1}^{N_L} c_j(h) \frac{(-h)^{|\alpha|} z_j^\alpha}{\alpha!} = a_\alpha, \quad |\alpha| \leq L. \quad (30)$$

The inverse Vandermonde matrix shows that $\max_j |c_j(h)| \leq C(q, L)h^{-L}$ for $0 < h \leq 1$. Taylor's formula for translations, taken in H^1 , gives

$$G(\cdot - h z_j) = \sum_{|\alpha| \leq L} \frac{(-h)^{|\alpha|} z_j^\alpha}{\alpha!} D^\alpha G + r_{j,L}(h), \quad \|r_{j,L}(h)\|_{H^1} \leq C(L, z_j)h^{L+1},$$

because $G \in H^m$ for every m . The moment equations cancel the Taylor polynomial against q , and hence

$$\|q_h - q\|_{H^1} \leq \sum_{j=1}^{N_L} |c_j(h)| \|r_{j,L}(h)\|_{H^1} \leq C(q, L)h \rightarrow 0.$$

□

The coefficient growth in Theorem 5.3 is not hidden: it is another instance of parameter escape. The lemma is an approximation statement, not a claim of numerical conditioning.

Proposition 5.4 (Weighted approximation rate). *There is $C_d > 0$ such that, for $v \in H^2(K)$ and $P \geq 2$,*

$$\inf_{w \in \mathcal{M}_P} \|v - w\|_{H^1(\mathbb{R}^d)} \leq C_d P^{-1/(2d)} \|v\|_{H^2(K)}. \quad (31)$$

Proof. Since $K \geq 1$, the unweighted H^1 -norm is bounded by the weighted one. For $P = N_L$, combine (29) with Theorem 5.3 and take the infimum over \mathcal{M}_{N_L} :

$$\inf_{w \in \mathcal{M}_{N_L}} \|v - w\|_{H^1} \leq C_d (L+1)^{-1/2} \|v\|_{H^2(K)}.$$

For general P , take the largest L such that $N_L \leq P$, pad with zero-weight neurons, and use $N_L \asymp_d (L+1)^d$. □

5.3 Localization to the whole space

Write

$$L_1^2(\mathbb{R}^d) := L^2(\mathbb{R}^d; (1 + |x|^2) dx), \quad \|f\|_{L_1^2}^2 := \int_{\mathbb{R}^d} (1 + |x|^2) |f(x)|^2 dx,$$

and

$$H_1^1(\mathbb{R}^d) := \{v \in H^1(\mathbb{R}^d) : v, \nabla v \in L_1^2(\mathbb{R}^d)\}, \quad \|v\|_{H_1^1}^2 := \int_{\mathbb{R}^d} (1 + |x|^2) (|v|^2 + |\nabla v|^2) dx.$$

Theorem 5.5 (Constructive whole-space rate). *There is a constant $C_d > 0$ such that, for $u \in H_1^1(\mathbb{R}^d) \cap H^2(\mathbb{R}^d)$ and $P \geq 2$,*

$$\inf_{w \in \mathcal{M}_P} \|u - w\|_{H^1(\mathbb{R}^d)} \leq \frac{C_d}{\sqrt{\log(2+P)}} (\|u\|_{H_1^1} + \|u\|_{H^2}). \quad (32)$$

Consequently, the relaxed states and near-minimizers in Theorem 5.1 satisfy the same state rate, with the additional optimization term shown in (27).

Proof. Choose $\varphi \in C_c^\infty(\mathbb{R}^d)$ such that $\varphi = 1$ on B_1 and $\varphi = 0$ outside B_2 . For $R \geq 1$, set $\varphi_R(x) = \varphi(x/R)$ and $u_R = u\varphi_R$. Direct differentiation and the weighted tail estimate give

$$\|u - u_R\|_{H^1} \leq \frac{C}{R} \|u\|_{H^1}. \quad (33)$$

The product rule gives $\|u_R\|_{H^2} \leq C\|u\|_{H^2}$, uniformly for $R \geq 1$. Since $\text{supp } u_R \subset B_{2R}$ and $K(x) \leq e^{R^2}$ on that ball,

$$\|u_R\|_{H^2(K)} \leq C e^{R^2/2} \|u\|_{H^2}. \quad (34)$$

By Theorem 5.4,

$$\inf_{w \in \mathcal{M}_P} \|u - w\|_{H^1} \leq \frac{C}{R} \|u\|_{H^1} + C e^{R^2/2} P^{-1/(2d)} \|u\|_{H^2}.$$

For sufficiently large P , take $R^2 = (2d)^{-1} \log P$. The second term is then $C P^{-1/(4d)} \|u\|_{H^2}$, which is bounded by the right-hand side of (32). Enlarging the constant covers the remaining finite range of P . \square

The regularity hypothesis follows from a natural weighted assumption on the source.

Lemma 5.6 (Weighted elliptic estimate). *If*

$$f \in L_1^2(\mathbb{R}^d)$$

then the solution of (9) belongs to $H_1^1(\mathbb{R}^d) \cap H^2(\mathbb{R}^d)$, and

$$\|u\|_{H_1^1} + \|u\|_{H^2} \leq C_d \|f\|_{L_1^2}. \quad (35)$$

Proof. Let $m(\xi) = (1 + |\xi|^2)^{-1}$. Then $\widehat{u} = m\widehat{f}$, and the unweighted H^2 -estimate follows because $(1 + |\xi|^2)m$ is bounded. The assumption $f \in L_1^2$ is equivalent, by Plancherel, to $\widehat{f} \in H^1(\mathbb{R}^d)$. The multipliers m , $\xi_j m$, and all of their first derivatives are bounded. Therefore

$$\nabla_\xi(m\widehat{f}), \quad \nabla_\xi(\xi_j m\widehat{f}), \quad j = 1, \dots, d,$$

belong to L^2 , with norms bounded by $C_d \|f\|_{L_1^2}$. A second application of Plancherel identifies these quantities with xu and $x \partial_j u$, respectively, and proves (35). \square

Combining Theorems 5.1, 5.5 and 5.6 gives the advertised PDE estimate.

Corollary 5.7 (Logarithmic state rate). *Assume $f \in L_1^2(\mathbb{R}^d)$. If u_P is a weak accumulation point of a fixed-width minimizing sequence as in Theorem 5.1, then*

$$\|u_P - u\|_{H^1} \leq \frac{C_d}{\sqrt{\log(2+P)}} \|f\|_{L_1^2}.$$

If $v_P \in \mathcal{M}_P$ satisfies $J(v_P) \leq I_P + \varepsilon_P$, then

$$\|v_P - u\|_{H^1} \leq \frac{C_d}{\sqrt{\log(2+P)}} \|f\|_{L_1^2} + \sqrt{2\varepsilon_P}.$$

Remark 5.8 (Perspective on sharpness). *The logarithmic estimate is a uniform whole-space rate on bounded subsets of $H_1^1(\mathbb{R}^d) \cap H^2(\mathbb{R}^d)$. Three features make this the natural scale at the level of generality considered here. First, the spectral step is sharp in the Hermite–Gaussian Hilbert scale:*

the tail from $H^2(K)$ to $H^1(K)$ has order $(L + 1)^{-1/2}$. Second, the realization step does not add an arbitrary discretization loss: the Hermite–Gaussian jet space

$$V_L = \text{span}\{D^\alpha G : |\alpha| \leq L\}$$

has dimension $N_L = \binom{L+d}{d}$, and Theorem 5.3 realizes an arbitrary element of this space with N_L colliding fixed-variance translates. This is the correct count for the uniform jet-realization mechanism used in the proof. Third, the passage from the unweighted whole-space setting to the exponential Hermite scale is made only through one polynomial moment, which produces the localization balance leading to $(\log P)^{-1/2}$.

This should not be confused with a pointwise optimality statement for each fixed target. If $u \in H_1^1(\mathbb{R}^d) \cap H^2(\mathbb{R}^d)$ is fixed, then the localization tail satisfies $\|u - u_R\|_{H^1} = o(R^{-1})$. The same construction therefore gives $o((\log P)^{-1/2})$ for that particular u . The logarithmic estimate is instead a uniform statement, with a constant depending only on the stated norms. We do not prove a matching minimax lower bound for the nonlinear class \mathcal{M}_P . Such a lower bound would have to exclude all target-dependent choices of centers and not only the Hermite projection followed by the uniform jet construction above. At this level of generality, and with the Gaussian variance fixed, no sharper uniform finite-width whole-space estimate should be expected without imposing additional decay, analyticity, variable scales, or a different approximation structure.

5.4 Diagonal near-minimizers

The state estimate also shows how to choose one element from each fixed-width minimizing sequence.

Proposition 5.9 (Selecting sufficiently accurate minimizing states). *For each P , let $(v_P^k)_{k \geq 1} \subset \mathcal{M}_P$ satisfy $J(v_P^k) \rightarrow I_P$ as $k \rightarrow \infty$.*

(a) *There is a diagonal choice $k(P)$ such that*

$$J(v_P^{k(P)}) \leq I_P + \frac{1}{\log(2+P)}. \quad (36)$$

If $f \in L_1^2(\mathbb{R}^d)$, then

$$\|v_P^{k(P)} - u\|_{H^1} \leq \frac{C_d(1 + \|f\|_{L_1^2})}{\sqrt{\log(2+P)}}. \quad (37)$$

(b) *More generally, if $z_P \in \mathcal{M}_P$ satisfies*

$$J(z_P) \leq I_P + \varepsilon + o(1)$$

for a fixed $\varepsilon \geq 0$, then

$$\limsup_{P \rightarrow \infty} \|z_P - u\|_{H^1} \leq \sqrt{2\varepsilon}. \quad (38)$$

Proof. For each P , convergence to I_P permits a choice satisfying (36). Estimates (37) and (38) follow from (27), $\delta_P \rightarrow 0$, and, in the first case, Theorems 5.5 and 5.6 above. \square

This selection is existential; it gives no bound on $k(P)$. Any width–iteration complexity estimate would require a separate analysis of the chosen training dynamics.

6 Measure-valued relaxation and regularization

6.1 A measure-valued relaxation of the finite-neuron problem

We now ask whether the loss of compactness observed for finite Gaussian mixtures disappears after passing to a measure-valued, convex relaxation of the problem. The idea is to replace the finite collection of weights and centers by a finite signed Radon measure. In this formulation, finite Gaussian mixtures are recovered by atomic measures, while general measures give a larger admissible class.

Let $\mathcal{M}(\mathbb{R}^d)$ denote the space of finite signed Radon measures, equipped with the total-variation norm. For $\mu \in \mathcal{M}(\mathbb{R}^d)$, define

$$v_\mu := G * \mu, \quad J_r(\mu) := J(v_\mu), \quad I_r := \inf_{\mu \in \mathcal{M}(\mathbb{R}^d)} J_r(\mu).$$

Young's inequality for measures gives $v_\mu \in H^1(\mathbb{R}^d)$. If

$$\mu = \sum_{j=1}^P w_j \delta_{x_j},$$

then

$$G * \mu = \sum_{j=1}^P w_j G(\cdot - x_j),$$

so the finite realization class \mathcal{M}_P corresponds to atomic measures with at most P atoms. Thus the problem defining I_r is a relaxed version of the finite-neuron problem.

The next result shows that the relaxation has the correct limiting state, but does not restore coercivity in the representing measures.

Proposition 6.1 (Relaxed minimizing states). *One has $I_r = I$. If $(\mu_k)_k$ is any minimizing sequence for I_r , then*

$$G * \mu_k \longrightarrow u \quad \text{strongly in } H^1(\mathbb{R}^d).$$

Moreover, there exist minimizing sequences whose total variation tends to infinity. Thus the relaxed energy does not, by itself, provide a total-variation bound on representing measures.

Proof. Clearly $I \leq I_r$, since I is the minimum of J over all of $H^1(\mathbb{R}^d)$. Conversely, atomic measures generate the dense union $\bigcup_P \mathcal{M}_P$, and therefore $I_r \leq I$. Hence $I_r = I$.

If $(\mu_k)_k$ is minimizing, then

$$J(G * \mu_k) \rightarrow J(u).$$

Using the energy identity (11), we obtain

$$\frac{1}{2} \|G * \mu_k - u\|_{H^1}^2 = J(G * \mu_k) - J(u) \rightarrow 0,$$

which proves the strong convergence of the realized states.

For the example $u = \partial_1 G$, the measures

$$\mu_h := \frac{\delta_{-he_1} - \delta_{he_1}}{2h}$$

satisfy

$$G * \mu_h = q_h \rightarrow \partial_1 G \quad \text{strongly in } H^1(\mathbb{R}^d),$$

whereas

$$\|\mu_h\|_{\text{TV}} = h^{-1} \rightarrow \infty.$$

These measures are therefore a minimizing sequence for $I_r = I$, but they are unbounded in total variation. \square

Thus the relaxation reproduces the limiting state, but the representing measures may still escape in total variation.

6.2 Fourier interpretation of relaxed noncoercivity

The preceding example reflects a simple Fourier mechanism: convolution with the Gaussian smooths the measure before the energy sees it. Indeed,

$$\widehat{v_\mu}(\xi) = e^{-|\xi|^2} \widehat{\mu}(\xi), \quad \widehat{\nabla v_\mu}(\xi) = i\xi e^{-|\xi|^2} \widehat{\mu}(\xi). \quad (39)$$

Consequently, an H^1 -bound on v_μ controls only

$$(1 + |\xi|^2)^{1/2} e^{-|\xi|^2} \widehat{\mu}(\xi) \quad \text{in } L^2(\mathbb{R}^d). \quad (40)$$

Because of the exponentially decaying factor, this estimate gives no bound on $\|\mu\|_{\text{TV}}$. In the collision example, $\widehat{\mu}_h(\xi) = i \sin(h\xi_1)/h$ converges pointwise to $i\xi_1$, while $\|\mu_h\|_{\text{TV}} \rightarrow \infty$. The state is therefore regularized by convolution, not by compactness of the representing measures.

Convexity of J_r in the measure variable removes the finite-particle center nonconvexity at the formal infinite-dimensional level. However, minimizing sequences may still leave every bounded total-variation set. Particle discretizations of the relaxed problem can therefore reproduce the same concentration mechanism as the original Gaussian parametrization; compare [1, 6, 34].

A total-variation penalty restores compactness at the measure level. For $\delta > 0$, define

$$J_\delta(\mu) := J(G * \mu) + \delta \|\mu\|_{\text{TV}}^2. \quad (41)$$

Proposition 6.2 (Existence for the regularized relaxed problem). *For every $\delta > 0$, J_δ attains its minimum on $\mathcal{M}(\mathbb{R}^d)$.*

Proof. Since $J \geq I$, every sublevel of J_δ is bounded in total variation. Banach–Alaoglu and the separability of $C_0(\mathbb{R}^d)$ give sequential weak-star compactness. If $\mu_k \rightharpoonup^* \mu$, then $G * \mu_k \rightarrow G * \mu$ in H^1 : testing against an H^1 -function produces a continuous function of the translation variable that vanishes at infinity. The weak lower semicontinuity of J and of the total-variation norm completes the direct-method argument. \square

The discrete counterpart adds

$$\delta \left(\sum_j |w_j| \right)^2$$

to the reduced loss. This controls colliding weights, but it does not control centers of inactive neurons, remove permutation symmetries, or make the center optimization convex. Moreover, fixed $\delta > 0$ biases the state, while the limit $\delta \downarrow 0$ may recover parameter escape.

7 Kernel choice, activation functions, and persistence of the gap

The Gaussian is exceptionally smoothing because its Fourier transform decays exponentially. A slower multiplier might improve the relation between parameter and state norms, but only if the associated convolution can be inverted stably in norms compatible with the PDE energy. We do not attempt a full characterization here.

One formal alternative is the Riesz kernel

$$H_\alpha(x) = |x|^{-\alpha}, \quad 0 < \alpha < d, \quad (42)$$

understood as a tempered distribution. Its Fourier transform is

$$\widehat{H}_\alpha(\xi) = C_{d,\alpha}|\xi|^{\alpha-d}.$$

It lies at the weak-Lebesgue endpoint $H_\alpha \in L^{d/\alpha,\infty}(\mathbb{R}^d)$, rather than in L^1 , so all convolution statements require the fractional-integration interpretation. If $v_\mu = H_\alpha * \mu$, then formally

$$|\widehat{\nabla v_\mu}(\xi)| = C_{d,\alpha}|\xi|^{\alpha-d+1}|\widehat{\mu}(\xi)|. \quad (43)$$

When $d \geq 2$, the choice $\alpha = d - 1$ makes the multiplier in (43) of order zero:

$$\widehat{\nabla v_\mu}(\xi) = C_{d,i} \frac{\xi}{|\xi|} \widehat{\mu}(\xi).$$

Thus, for an L^2 -density μ , the homogeneous energy $\|\nabla v_\mu\|_{L^2}$ is comparable to $\|\mu\|_{L^2}$ by the boundedness of the Riesz transforms. This is much less smoothing than the Gaussian map.

It does not, however, yield a coercive parametrization of the full $H^1(\mathbb{R}^d)$ -norm. The L^2 -part of the state requires

$$|\xi|^{-1}\widehat{\mu}(\xi) \in L^2(\mathbb{R}^d),$$

which creates a low-frequency obstruction; finite measures need not possess L^2 -densities; and H_{d-1} is not an L^1 -activation. Riesz kernels therefore trade Gaussian high-frequency smoothing for low-frequency and domain difficulties. They are an instructive comparison, not a ready-made remedy.

The collision mechanism is not restricted to Gaussians. If a smooth activation σ and its derivative belong to the chosen state space, then

$$\frac{\sigma(\cdot + h) - \sigma(\cdot - h)}{2h} \longrightarrow \sigma'$$

in that space under the corresponding translation-continuity assumptions. If σ' is not contained in the fixed realization class, the class is again nonclosed.

For deep architectures the activation, architecture, domain, and topology have to be checked separately. The Gaussian construction should therefore be read as a model mechanism, not as a theorem for all networks. In a given deep architecture, an analogous argument would require showing that a colliding configuration in one layer produces a limiting feature, such as a derivative or first-order variation of an activation profile, and that the subsequent layers propagate this limit continuously. The relevant continuity, stability, and nondegeneracy properties are architecture-dependent.

Likewise, variable-coefficient elliptic equations, nonlinear variational problems, bounded domains, and evolution equations can retain the coercivity gap whenever their state functional is coercive but their realization map has noncompact fibers or a nonclosed image. The abstract theorem in Section 2 distinguishes this PDE stability statement from the architecture-specific realization analysis.

8 Residual minimization and state-space hybrid modelling

8.1 Residual minimization and PINNs

The coercivity gap is not specific to energy minimization. It also appears in residual-based methods, including Physics-Informed Neural Networks (PINNs) and variational PINN formulations [33]. In that setting, the loss may control the realized state through a PDE stability estimate, while

giving no coercive control of the neural parameters. The relevant question for the physical approximation is therefore the stability of the residual norm, not compactness of a particular parameter representation.

For the model operator

$$A = -\Delta + I : H^1(\mathbb{R}^d) \rightarrow H^{-1}(\mathbb{R}^d),$$

endow $H^{-1}(\mathbb{R}^d)$ with the dual norm induced by the H^1 -energy inner product. Then A is the Riesz isometry. Hence, if u solves $Au = f$, then

$$\mathcal{R}(v) := \|Av - f\|_{H^{-1}}^2 = \|v - u\|_{H^1}^2. \quad (44)$$

Thus residual minimization in the H^{-1} -stability norm is exactly state-error minimization in H^1 . In particular, if

$$\mathcal{R}(v_P) \leq \inf_{w \in \mathcal{M}_P} \mathcal{R}(w) + \eta_P,$$

then

$$\|v_P - u\|_{H^1}^2 \leq \inf_{w \in \mathcal{M}_P} \|w - u\|_{H^1}^2 + \eta_P. \quad (45)$$

Consequently, the approximation results obtained above for the Gaussian realization classes immediately transfer to this residual formulation: small residual implies convergence of the realized states, but not boundedness of the representing parameters.

This is the residual form of the same separation. The PDE stability norm controls the physical error $v_P - u$, whereas the neural parametrization may still approach collision strata, exhibit weight blow-up, or otherwise lose compactness.

The choice of residual norm is essential. A pointwise, empirical, or collocation PINN loss is not automatically equivalent to the continuous H^{-1} -stability norm. Such a loss yields state convergence only when it is connected to the continuous residual by an additional sampling, quadrature, or discrete stability estimate. Similarly, an L^2 -residual controls a stronger regularity framework: if $f \in L^2(\mathbb{R}^d)$, then $A : H^2(\mathbb{R}^d) \rightarrow L^2(\mathbb{R}^d)$ is an isomorphism and

$$\|v - u\|_{H^2} \leq C \|Av - f\|_{L^2}.$$

Here the trial functions must belong to the L^2 -operator domain, and the regularity estimate must hold for the equation and domain under consideration. These distinctions do not remove the parameter–state separation: even when the residual guarantees convergence of the computed states in H^2 , it need not yield compactness of the corresponding parameters.

8.2 A state-space HYCO formulation for hybrid physics–data modelling

We have so far considered two purely physics-based variational principles: energy minimization and residual minimization. In many computational settings, however, the loss also contains a data-misfit term, for instance when the PDE model is combined with a finite number of measurements. We refer to such functionals as hybrid physics–data losses.

The HYCO viewpoint [16, 17] is useful independently of the parameter-coercivity issue: the physical model, the learned source, the synthetic state, and the observations are coupled at the state level. The purpose of this subsection is to formulate this coupling in Hilbert norms compatible with PDE stability. The coercivity-gap discussion then adds a separate warning: stability of the hybrid state problem does not by itself imply compactness of the finite parameters used to represent its components.

Point evaluation is not continuous on $H^1(\mathbb{R}^d)$ for $d \geq 2$. Thus, when the hybrid loss is formulated at the energy level, point measurements should be replaced by bounded observation functionals, for instance local averages,

$$\ell_i(v) = \int_{\mathbb{R}^d} \rho_i v \, dx, \quad \rho_i \in L^2(\mathbb{R}^d),$$

or, more generally,

$$\ell_i(v) = \langle \rho_i, v \rangle_{H^{-1}, H^1}, \quad \rho_i \in H^{-1}(\mathbb{R}^d).$$

This is also closer to physical measurements, which usually average the state over a nonzero sensor volume. Genuine point observations are admissible only when the state space has enough regularity to embed into C^0 . In particular, in residual minimization measured in L^2 , where the natural state regularity is H^2 , point observations are continuous in dimensions $d \leq 3$.

To recover the concrete finite-particle representation used in hybrid physics–data methods, one may employ independent Gaussian mixtures for the source, physical state, and synthetic state:

$$\begin{aligned} f_{*,P}(x) &= \sum_{j=1}^P f_j G(x - x_{f,j}), \\ u_{\text{phy},P}(x) &= \sum_{j=1}^P p_j G(x - x_{p,j}), \\ u_{\text{syn},P}(x) &= \sum_{j=1}^P s_j G(x - x_{s,j}). \end{aligned} \tag{46}$$

The corresponding parameter vector is

$$\Theta_P = ((f_j, x_{f,j}), (p_j, x_{p,j}), (s_j, x_{s,j}))_{j=1}^P.$$

Using a common width is only a notational convenience; the three widths may be chosen independently. The loss below is evaluated on the realizations in (46), while the observations remain bounded functionals rather than ill-defined point values in H^1 .

For data $y_i \in \mathbb{R}$, $\nu > 0$, and $\lambda > 0$, consider

$$\begin{aligned} \mathcal{L}(f_*, u_{\text{phy}}, u_{\text{syn}}) &:= \frac{1}{2} \|Au_{\text{phy}} - f_*\|_{H^{-1}}^2 + \frac{\nu}{2} \|f_*\|_{H^{-1}}^2 \\ &+ \frac{1}{2N} \sum_{i=1}^N |\ell_i(u_{\text{syn}}) - y_i|^2 + \frac{\lambda}{2} \|u_{\text{phy}} - u_{\text{syn}}\|_{H^1}^2. \end{aligned} \tag{47}$$

Proposition 8.1 (Well-posed hybrid state problem). *The functional \mathcal{L} is continuous, coercive, and strongly convex on*

$$H^{-1}(\mathbb{R}^d) \times H^1(\mathbb{R}^d) \times H^1(\mathbb{R}^d).$$

It therefore has a unique minimizer. If all three components are approximated by increasing finite Gaussian spans and the computed triples are globally near-minimizing with optimization error tending to zero, then their realized states converge strongly to this minimizer in the product space.

Proof. Let $z = (f_*, u_{\text{phy}}, u_{\text{syn}})$. The positive quadratic part of \mathcal{L} , without the observation term, is

$$Q(z) := \frac{1}{2} \|Au_{\text{phy}} - f_*\|_{H^{-1}}^2 + \frac{\nu}{2} \|f_*\|_{H^{-1}}^2 + \frac{\lambda}{2} \|u_{\text{phy}} - u_{\text{syn}}\|_{H^1}^2.$$

It controls the product norm. Indeed, f_* is controlled by the ν -term, and the Riesz-isometry property of A gives

$$\|u_{\text{phy}}\|_{H^1} \leq \|Au_{\text{phy}} - f_*\|_{H^{-1}} + \|f_*\|_{H^{-1}},$$

while

$$\|u_{\text{syn}}\|_{H^1} \leq \|u_{\text{syn}} - u_{\text{phy}}\|_{H^1} + \|u_{\text{phy}}\|_{H^1}.$$

Consequently there is $c_{\nu,\lambda} > 0$ such that

$$Q(z) \geq c_{\nu,\lambda} (\|f_*\|_{H^{-1}}^2 + \|u_{\text{phy}}\|_{H^1}^2 + \|u_{\text{syn}}\|_{H^1}^2).$$

The observation term is continuous and convex because the ℓ_i are bounded. Hence \mathcal{L} is coercive and strongly convex on the product space. Existence and uniqueness follow by the direct method. Gaussian spans are dense in H^1 , and consequently also dense in H^{-1} ; the convergence assertion is Theorem 2.1 applied in the product space. \square

The proposition is stated for the global minimization problem, but the same state-space principle is the one used in HYCO-type formulations, once combined with the descent or convergence properties of the corresponding alternating updates. Thus the hybrid model is not introduced here as a remedy for parameter noncoercivity. It is a stable state-level way of coupling physics, data, and learned components. The additional message of the present paper is that this stability controls the realized triple $(f_*, u_{\text{phy}}, u_{\text{syn}})$, but not necessarily the finite-dimensional parameterization Θ_P . Strong convergence of the realized hybrid states can therefore coexist with escape of the parameters representing them.

9 Scope, limitations, and open directions

The results of this paper isolate a general mechanism: variational neural PDE solvers may be coercive in the realized state while remaining non-coercive in the parameters. This coercivity gap is not specific to the Gaussian model used above. The present construction provides a transparent PDE setting in which the phenomenon can be proved completely, but the same state-versus-parameter distinction is intrinsic to many neural and particle-based approximation schemes. The following directions indicate where the mechanism should be made explicit in further settings.

- **Architecture.** The proofs have been written for a shallow, fixed-variance Gaussian radial-basis class in order to display the mechanism in its simplest form. Smooth activations can generate analogous difference-quotient collisions, and fixed-size realization sets are often nonclosed [31]. For each concrete deep architecture, however, the corresponding statement has to be proved from the realization map and from the noncompact parameter directions that leave the realized state convergent.
- **Optimization.** The state estimates are formulated for globally near-minimizing sequences. This is the natural variational level at which the coercivity gap appears. Algorithmic training adds a second layer: one has to quantify how gradient, alternating, or regularized dynamics approach such near-minimizers. This does not change the state-versus-parameter mechanism; it determines which minimizing or near-minimizing sequences are actually produced by a given optimization method.
- **Approximation rates.** The estimates obtained here are natural, and essentially sharp, when viewed from the Gaussian–Hermite spectral construction on which the proof is based. Their deterioration in the Sobolev setting comes from the passage from this spectral framework to estimates involving only one moment of the target function. Whether this loss is intrinsic to the approximation class, or can be reduced by a more refined argument, remains an open question. Faster rates require additional structure on the target, for instance stronger decay, analyticity, adaptive scaling properties, or membership in dimension-robust approximation spaces such as spectral Barron classes [5].

- **Qualitative PDE structure.** The coercivity gap also interacts with qualitative PDE properties. For $f \geq 0$, the exact solution of (9) is nonnegative, but an unrestricted signed Gaussian mixture need not be. Moreover, $v \in \mathcal{M}_P$ does not imply $v^+ \in \mathcal{M}_P$, so the standard variational argument based on replacing a competitor by its positive part cannot be performed inside \mathcal{M}_P . This shows that preserving comparison principles, positivity, or maximum principles requires realization classes designed to encode these structures while retaining approximation power.
- **Numerical design.** The phenomenon identified here provides a criterion for numerical design: methods should monitor state accuracy first, in norms dictated by PDE stability. Parameter norms and conditioning should also be recorded, but they should be interpreted as diagnostics of the representation and the optimizer, not as substitutes for the physical error. Freezing or regularizing centers converts part of the problem into a stable linear approximation, but it also reduces adaptivity. Frozen centers may be drawn as random features or selected through quantization and Voronoi procedures such as Lloyd’s algorithm [23]. A systematic comparison of adaptive centers, random features, and deterministic radial-basis designs should therefore track state errors, residuals, parameter norms, conditioning, and computational cost.
- **Renormalization of escaping parameters.** When parameter escape occurs, it may still be possible to extract useful information from the escaping configuration by a suitable renormalization, in the spirit of blow-up analysis for PDEs. For Gaussian classes, collisions of centers and diverging amplitudes can produce derivative-type limiting profiles through difference-quotient mechanisms. Such a procedure would not remove the coercivity gap, since the original parameters remain noncompact, but it could help identify the compactified representation underlying the convergent state. Developing numerical renormalization strategies for such escaping minimizing sequences remains an open direction.
- **Hybrid methods.** HYCO-type losses should also be viewed as hybrid modelling tools in their own right. The well-posed state functional in Theorem 8.1 shows that the realized source, physical state, and synthetic state can be coupled and controlled in the natural product space. The coercivity-gap analysis is a separate qualification: this state control does not make the underlying finite-dimensional parameters coercive. The remaining work is to write the corresponding algorithmic analysis for alternating HYCO-type updates, including the role of coupling and regularization parameters, concentration in the three realization classes, and noisy or incomplete observations.

10 Conclusion

This paper isolates a coercivity gap that is easy to miss in neural PDE methods. A coercive PDE energy controls the realized physical state, but it need not control the parameters used to represent that state. In the Gaussian elliptic model this separation is complete: two active neurons collide, the reduced minimum is not attained, and every exact minimizing parameter sequence escapes, while the corresponding realized states converge strongly in the energy norm.

The example should be read as a structural diagnosis rather than as a universal divergence statement. If the exact solution already belongs to a finite Gaussian class, as for a single Gaussian or a finite Gaussian mixture with sufficient width, no boundary chase is forced. Parameter escape occurs here because the chosen solution lies in the H^1 -closure of each finite realization class but outside the class itself. The ansatz is therefore rich enough to approximate the state arbitrarily well, but only through parameter sequences that move toward a boundary point with no finite representative.

The broader methodological message is that neural PDE solvers should be analyzed first as state-space approximation methods and only then as finite-dimensional parameter optimizations. The parameters are the coordinates used by the algorithm; the PDE sees the realized state. In nonclosed realization classes these two levels may separate: the state may converge in the coercive PDE norm while every exact minimizing parameter sequence escapes. This does not invalidate neural PDE solvers. It explains why they can perform well at the level of physical fields even when the associated parameter dynamics are unstable, nonunique, or poorly conditioned.

For computations, the first validation criterion should therefore be the state error when it is available, and otherwise computable proxies such as energy gaps, stability-norm residuals, or observation errors. Parameter convergence, boundedness, and conditioning remain important, but they are secondary diagnostics rather than the primary notion of PDE accuracy. Residual, relaxed, and hybrid formulations fit the same viewpoint when their norms are compatible with PDE stability. Parameter regularization can restore compactness, but it also introduces bias and leaves the nonconvex training problem in place. The lesson is both cautionary and positive: parameter compactness should not be assumed, but state convergence can still be proved and should be the central object of analysis.

Acknowledgments

The author thanks Antonio Álvarez-López (Universidad Autónoma de Madrid) and Daniel Fernández (Friedrich–Alexander–Universität Erlangen–Nürnberg) for fruitful discussions.

The author was funded by the Alexander von Humboldt Professorship program, the ERC Advanced Grant CoDeFeL, Grant PID2023-146872OB-I00-DyCMod of MICIU (Spain), COST Actions CA24136 (InterCoML) and CA24122 (mSPACE), supported by COST (European Cooperation in Science and Technology), project AFOSR 24IOE027, and SURE-AI Centre grant 357482 of the Research Council of Norway.

A Technical complements for the weighted Gaussian approximation

This appendix records the weighted spectral and localization details that underlie Section 5. The same self-similar operator appears in the large-time analysis of the heat equation and in moment methods for inverse problems; see [42, 22].

A.1 The self-similar elliptic operator

Recall

$$K(x) = e^{|x|^2/4}, \quad \mathcal{L} = -\Delta - \frac{x \cdot \nabla}{2} = -K^{-1} \operatorname{div}(K \nabla).$$

The weighted scalar product is

$$(v, w)_K := \int_{\mathbb{R}^d} v(x)w(x)K(x) \, dx.$$

Proposition A.1 (Weighted spectral framework). *The operator \mathcal{L} has the following properties.*

- (i) *The embedding $H^1(K) \hookrightarrow L^2(K)$ is compact.*
- (ii) *The form $a(v, w) = \int_{\mathbb{R}^d} \nabla v \cdot \nabla w K \, dx$ defines a positive self-adjoint realization of \mathcal{L} with compact resolvent. Equivalently, $\mathcal{L} : H^1(K) \rightarrow H^1(K)'$ is an isomorphism when the spaces are equipped with the equivalent form norms.*

(iii) The eigenvalues, indexed by total derivative order $n \geq 0$, are

$$\mu_n = \frac{d+n}{2},$$

and the associated eigenspace is

$$E_n = \text{span}\{D^\alpha e^{-|x|^2/4} : |\alpha| = n\}.$$

(iv) After normalization, these eigenfunctions form an orthonormal basis of $L^2(K)$ and an orthogonal basis in the corresponding weighted Sobolev scales.

Proof. The divergence identity gives symmetry and the form relation

$$(\mathcal{L}v, v)_K = \int_{\mathbb{R}^d} |\nabla v|^2 K \, dx.$$

The weighted Poincaré inequality and the growth of K yield coercivity and compactness. Direct differentiation shows that the Gaussian derivatives are eigenfunctions with the displayed eigenvalues. Completeness follows after conjugating \mathcal{L} by $K^{1/2}$, which reduces it to a shifted harmonic oscillator. These standard facts, including the equivalence of the integer spectral and derivative norms, are detailed in [42]. \square

If $v = \sum_{n \geq 0} \pi_n v$ is the resulting spectral expansion and $v_L = \sum_{n=0}^L \pi_n v$, then

$$\begin{aligned} \|v - v_L\|_{H^1(K)}^2 &\leq C_d \sum_{n>L} (1 + \mu_n) \|\pi_n v\|_{L^2(K)}^2 \\ &\leq \frac{C_d}{1 + \mu_{L+1}} \sum_{n>L} (1 + \mu_n)^2 \|\pi_n v\|_{L^2(K)}^2 \\ &\leq \frac{C_d}{L+1} \|v\|_{H^2(K)}^2. \end{aligned}$$

Taking square roots gives precisely the $(L+1)^{-1/2}$ norm rate used in (29). The square root is essential; omitting it would lead to the incorrect exponent $P^{-1/d}$.

A.2 Detailed localization estimates

Let $\varphi \in C_c^\infty(\mathbb{R}^d)$ satisfy

$$0 \leq \varphi \leq 1, \quad \varphi = 1 \text{ on } B_1, \quad \varphi = 0 \text{ outside } B_2,$$

and set $\varphi_R(x) = \varphi(x/R)$, $u_R = u\varphi_R$. Then

$$u - u_R = (1 - \varphi_R)u, \quad \nabla(u - u_R) = (1 - \varphi_R)\nabla u - u\nabla\varphi_R.$$

Since $\nabla\varphi_R$ is supported in $B_{2R} \setminus B_R$ and $\|\nabla\varphi_R\|_\infty \leq C/R$,

$$\begin{aligned} \|u - u_R\|_{H^1} &\leq \|u\|_{L^2(\mathbb{R}^d \setminus B_R)} + \|\nabla u\|_{L^2(\mathbb{R}^d \setminus B_R)} \\ &\quad + \frac{C}{R} \|u\|_{L^2(B_{2R} \setminus B_R)}. \end{aligned}$$

If $u \in H_1^1$, multiplication by $|x| \geq R$ on the exterior region gives

$$\|u - u_R\|_{H^1} \leq \frac{C}{R} \|u\|_{H_1^1}.$$

For $|\alpha| \leq 2$, the product rule gives

$$D^\alpha u_R = \sum_{\beta \leq \alpha} \binom{\alpha}{\beta} D^\beta u D^{\alpha-\beta} \varphi_R, \quad \|D^\gamma \varphi_R\|_\infty \leq C_\gamma R^{-|\gamma|}.$$

Consequently, for $R \geq 1$,

$$\|u_R\|_{H^2} \leq C(\|u\|_{H^2} + R^{-1}\|u\|_{H^1} + R^{-2}\|u\|_{L^2}) \leq C\|u\|_{H^2}.$$

Finally, $\text{supp } u_R \subset B_{2R}$ and $K(x) \leq e^{R^2}$ on this ball, so

$$\|u_R\|_{H^2(K)} \leq C e^{R^2/2} \|u\|_{H^2}.$$

Combining these three estimates with Theorem 5.4 produces

$$\inf_{w \in \mathcal{M}_P} \|u - w\|_{H^1} \leq \frac{C}{R} \|u\|_{H^1} + C e^{R^2/2} P^{-1/(2d)} \|u\|_{H^2},$$

from which (32) follows by the choice made in Theorem 5.5.

A.3 An alternative weighted energy argument

The Fourier proof of Theorem 5.6 is concise, but the weighted H^1 -estimate can also be obtained directly from the PDE. This derivation is useful for variable-coefficient problems where an explicit Fourier multiplier is unavailable.

Choose bounded smooth weights ρ_R increasing pointwise to $1 + |x|^2$ and satisfying, uniformly in R ,

$$1 \leq \rho_R \leq 1 + |x|^2, \quad |\nabla \rho_R|^2 \leq C \rho_R. \quad (48)$$

Such weights are obtained by smoothly truncating $1 + |x|^2$ at height $1 + R^2$. Since ρ_R and its gradient are bounded, $\rho_R u$ is an admissible test function in the weak equation. We obtain

$$\int_{\mathbb{R}^d} \rho_R (|\nabla u|^2 + |u|^2) dx = \int_{\mathbb{R}^d} \rho_R f u dx - \int_{\mathbb{R}^d} u \nabla u \cdot \nabla \rho_R dx. \quad (49)$$

For arbitrary $\varepsilon > 0$, Young's inequality and (48) give

$$\begin{aligned} \left| \int \rho_R f u \right| &\leq \frac{1}{4} \int \rho_R |u|^2 + C \int (1 + |x|^2) |f|^2, \\ \left| \int u \nabla u \cdot \nabla \rho_R \right| &\leq \varepsilon \int \rho_R |\nabla u|^2 + C_\varepsilon \int |u|^2. \end{aligned}$$

Choosing ε small and using the unweighted energy estimate to control $\|u\|_{L^2}$, we find

$$\int_{\mathbb{R}^d} \rho_R (|\nabla u|^2 + |u|^2) dx \leq C \|f\|_{L^2_1}^2, \quad (50)$$

with C independent of R . Monotone convergence (or Fatou's lemma for a nonmonotone smooth truncation) yields $u \in H^1_1$. The unweighted H^2 -bound still follows from elliptic regularity. This proves (35) without differentiating the Fourier transform of f .

A.4 Explicit derivative stencils and shared neuron counts

The space of Gaussian derivatives of total order at most L has dimension $N_L = \binom{L+d}{d}$. Theorem 5.3 uses exactly N_L distinct translates to approximate an arbitrary element of this space. The connection with familiar finite differences is easiest to see in one dimension. For $m \geq 1$, define

$$D_{h,m}G(x) := \frac{1}{h^m} \sum_{j=0}^m (-1)^{m-j} \binom{m}{j} G\left(x + \left(j - \frac{m}{2}\right)h\right). \quad (51)$$

Then

$$D_{h,m}G \longrightarrow G^{(m)} \quad \text{in } H^1(\mathbb{R}) \quad \text{as } h \downarrow 0. \quad (52)$$

For example, $m = 1$ is the two-neuron collision used in Section 4, while $m = 2$ gives the three-point stencil

$$\frac{G(x+h) - 2G(x) + G(x-h)}{h^2} \longrightarrow G''(x).$$

To prove (52), one may use Taylor's formula in H^1 , or observe that the Fourier multiplier of (51) converges to $(i\xi)^m$ and is dominated by $|\xi|^m$; the Gaussian supplies every required moment.

For a multi-index α , tensorizing the one-dimensional stencil uses $\prod_{r=1}^d (\alpha_r + 1)$ translates to approximate $D^\alpha G$. Approximating every derivative separately would repeat many centers and would not give the sharp count N_L . The unisolvent construction in Theorem 5.3 instead selects N_L nodes once and solves the moment system for the entire polynomial jet. It thereby shares the same colliding centers among all derivatives of total order at most L .

For fixed L , the finite-difference step h may be chosen after the spectral projection so that the jet-realization error is arbitrarily small. The coefficients can nevertheless grow like h^{-L} , and the inverse Vandermonde constant depends on the selected nodes. Thus the construction proves a best-approximation bound with a controlled neuron count, but not a uniformly conditioned algorithm or a width-iteration complexity bound. This is precisely the distinction between expressive approximation and stable parameter recovery emphasized throughout the paper.

References

- [1] F. Bach, *Breaking the curse of dimensionality with convex neural networks*, J. Mach. Learn. Res. **18** (2017), 1–53.
- [2] N. Bellomo, F. Brezzi and E. Zuazua, *New trends in mathematics for scientific machine learning*, Math. Models Methods Appl. Sci. **36** (2026), no. 8, 1615–1621, doi:10.1142/S0218202526020033.
- [3] S. Bertoluzza, E. Burman and C. He, *WAN discretization of PDEs: Best approximation, stabilization, and essential boundary conditions*, SIAM J. Sci. Comput. **46** (2024), C688–C715.
- [4] M. D. Buhmann, *Radial basis functions*, Acta Numer. **9** (2000), 1–38.
- [5] Z. Chen, L. Huang, M. Yang and S. Zhou, *Regularity of second-order elliptic PDEs in spectral Barron spaces*, arXiv:2602.19381, 2026.
- [6] L. Chizat and F. Bach, *On the global convergence of gradient descent for over-parameterized models using optimal transport*, Adv. Neural Inf. Process. Syst. **31** (2018), 3036–3046.
- [7] G. Dal Maso, *An Introduction to Γ -Convergence*, Progress in Nonlinear Differential Equations and Their Applications, vol. 8, Birkhäuser, Boston, 1993.
- [8] T. De Ryck, A. D. Jagtap and S. Mishra, *Error estimates for physics-informed neural networks approximating the Navier–Stokes equations*, IMA J. Numer. Anal. **44** (2024), 83–119.

- [9] N. Doumèche, G. Biau and C. Boyer, *On the convergence of physics-informed neural networks*, Bernoulli **31** (2025), 2127–2151.
- [10] P. Dondl, J. Müller and M. Zeinhofer, *Uniform convergence guarantees for the Deep Ritz method for nonlinear problems*, Adv. Contin. Discrete Models **2022** (2022), article 49.
- [11] W. E and B. Yu, *The Deep Ritz method: A deep learning-based numerical algorithm for solving variational problems*, Commun. Math. Stat. **6** (2018), 1–12.
- [12] D. Fernández and E. Zuazua, *Quantitative conditioning and parameter escape for Gaussian neural PDE solvers*, work in preparation.
- [13] D. Gazoulis, I. Gkanis and C. G. Makridakis, *On the stability and convergence of physics informed neural networks*, IMA J. Numer. Anal. (2025), article draf090, doi:10.1093/imanum/draf090.
- [14] F. Girosi and T. Poggio, *Networks and the best approximation property*, Biol. Cybern. **63** (1990), 169–176.
- [15] L. I. Ignat and E. Zuazua, *Optimal convergence rates for the finite element approximation of the Sobolev constant* arXiv:2504.09637, (2025), Foundations of Computational Mathematics, to appear.
- [16] L. Liverani, T. Steynberg and E. Zuazua, *HYCO: Hybrid-cooperative learning for data-driven PDE modeling*, arXiv:2509.14123, 2025.
- [17] L. Liverani and E. Zuazua, *HYCO: A formalism for hybrid-cooperative PDE modelling*, arXiv:2602.23859, 2026.
- [18] P. C. Kainen, V. Kůrková and A. Vogt, *Approximation by neural networks is not continuous*, Neurocomputing **29** (1999), 47–56.
- [19] G. E. Karniadakis, I. G. Kevrekidis, L. Lu, P. Perdikaris, S. Wang and L. Yang, *Physics-informed machine learning*, Nat. Rev. Phys. **3** (2021), 422–440.
- [20] A. Langer, *Non-uniqueness of solutions in neural variational methods*, arXiv:2605.08877, 2026.
- [21] Q.-T. Le, R. Gribonval and E. Riccietti, *Does a sparse ReLU network training problem always admit an optimum?*, Adv. Neural Inf. Process. Syst. **36** (2023).
- [22] K. Liu and E. Zuazua, *Moments, time inversion and source identification for the heat equation*, Inverse Problems **42** (2026), 015009.
- [23] S. Lloyd, *Least squares quantization in PCM*, IEEE Trans. Inform. Theory **28** (1982), 129–137.
- [24] T. Luo, Z.-Q. J. Xu, Z. Ma and Y. Zhang, *Phase diagram for two-layer ReLU neural networks at infinite-width limit*, J. Mach. Learn. Res. **22** (2021), 1–47.
- [25] T. Luo and H. Yang, *Two-layer neural networks for partial differential equations: Optimization and generalization theory*, Handbook Numer. Anal. **25** (2024), 515–554.
- [26] W. R. Madych and S. A. Nelson, *Bounds on multivariate polynomials and exponential error estimates for multiquadric interpolation*, J. Approx. Theory **70** (1992), 94–114.
- [27] S. Mahan, E. J. King and A. Cloninger, *Nonclosedness of sets of neural networks in Sobolev spaces*, Neural Netw. **137** (2021), 85–96.
- [28] S. Mishra and R. Molinaro, *Estimates on the generalization error of physics-informed neural networks for approximating PDEs*, IMA J. Numer. Anal. **43** (2023), 1–43.
- [29] J. Müller and M. Zeinhofer, *Deep Ritz revisited*, arXiv:1912.03937, 2019.
- [30] J. Müller and M. Zeinhofer, *Achieving high accuracy with PINNs via energy natural gradient descent*, Proc. Mach. Learn. Res. **202** (2023), 25471–25485.

- [31] P. Petersen, M. Raslan and F. Voigtlaender, *Topological properties of the set of functions generated by neural networks of fixed size*, *Found. Comput. Math.* **21** (2021), 375–444.
- [32] M. Raissi, P. Perdikaris and G. E. Karniadakis, *Physics-informed neural networks: A deep learning framework for solving forward and inverse problems involving nonlinear partial differential equations*, *J. Comput. Phys.* **378** (2019), 686–707.
- [33] S. Rojas, P. Maczuga, J. Muñoz-Matute, D. Pardo and M. Paszyński, *Robust variational physics-informed neural networks*, *Comput. Methods Appl. Mech. Engrg.* **425** (2024), 116904, doi:10.1016/j.cma.2024.116904.
- [34] P. Savarese, I. Evron, D. Soudry and N. Srebro, *How do infinite width bounded norm networks look in function space?*, *Proc. Mach. Learn. Res.* **99** (2019), 2667–2690.
- [35] Y. Shin, J. Darbon and G. E. Karniadakis, *On the convergence of physics-informed neural networks for linear second-order elliptic and parabolic type PDEs*, *Commun. Comput. Phys.* **28** (2020), 2042–2074.
- [36] S. Wang, S. Sankaran, H. Wang and P. Perdikaris, *An expert’s guide to training physics-informed neural networks*, arXiv:2308.08468, 2023.
- [37] H. Wendland, *Scattered Data Approximation*, Cambridge University Press, Cambridge, 2005.
- [38] N. Wiener, *Tauberian theorems*, *Ann. of Math.* **33** (1932), 1–100.
- [39] H. Zhou, Q. Zhou, T. Luo, Y. Zhang and Z.-Q. J. Xu, *Towards understanding the condensation of neural networks at initial training*, *Adv. Neural Inf. Process. Syst.* **35** (2022), 2184–2196.
- [40] W. Zhao and T. Luo, *Convergence guarantees for gradient-based training of neural PDE solvers: From linear to nonlinear PDEs*, arXiv:2505.14002, 2025.
- [41] E. Zuazua, *Propagation, observation, and control of waves approximated by finite difference methods*, *SIAM Rev.* **47** (2005), 197–243.
- [42] E. Zuazua, *Asymptotic behavior of scalar convection–diffusion equations*, arXiv:2003.11834, 2020.